JCTC Journal of Chemical Theory and Computation

Nature of the Carbon−Sulfur Bond in the Species H−CS−OH

Henry S. Rzepa*

Department of Chemistry, Imperial College London, South Kensington Campus, London, SW7 2AZ, United Kingdom

Received August 20, 2010

Ⓦ **This paper contains enhanced objects available on the Internet at http://pubs.acs.org/JCTC.**

Abstract: A QTAIM (Quantum-Theory-Atoms-in-Molecules) and ELF (electron localization function) topological analysis of the bonding in the recently reported molecule HCSX, X = OH reveals that the central carbon−sulfur bond is highly tunable, from having triple character at one limit to being almost a single bond at the other depending on the nature of the group X.

The nature of bonding, and in particular the degree of multiple bonding between particular pairs of atoms continues to attract much attention from experimentalists, theoreticians, and increasingly from groups which exploit the synergies between both. Such an example appeared recently documenting the preparation, spectroscopic characterization and theoretical analysis of the species H−CS−X (**1**, *X* = OH).[1] The focus was on the nature of the carbon−sulfur bond, and its multiple-bonded character. The conclusion drawn from various types of analysis of the computed wave function and comparison with measured stretching frequencies was that the species exhibits a "*rather strong C═S double bond, or a weak C≡S triple bond*".[1] In this communication, I suggest that the multiple character of this carbon−sulfur bond can in fact be uniquely tuned across an unusually wide range simply by variation of the group X in **1**.

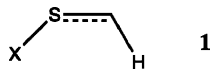

1

The original analysis[1] was based, inter alia, on comparison of measured C−S stretching frequencies with force constants computed at the CCSD (T)/cc-pVTZ level. Analysis of the wave function was provided at this level by inspection of individual molecular orbitals and localized NBO analysis of the bond orders, and by comparison with the diatomic species CS itself. Two methods that were not included in the original discussion[1] were those based on the topological properties of the electron density (QTAIM)[2] and analysis of the electron localization function (ELF) η.[3,4] These methods can often provide illuminating and complementary insights into the nature of bonding,[5] and they formed the basis for a discussion of the original article[1] on Bachrach's blog.[6] The discussion continued on this author's own blog,[7] with a formal outcome which includes further computational analysis being presented here.

The QTAIM method identifies, inter alia, the coordinates of a particular type of saddle-point in the electron density distribution ($\rho(r)$, which can be either computed as here, or measured experimentally) and which is known as a bond critical point, henceforth referred to as a BCP. Three electronic properties at the BCP are commonly used to characterize the nature of the bonding in this region; the value of $\rho(r)$ itself, the bond ellipticity ε[8], and the Laplacian $\nabla^2\rho(r)$. The magnitude of $\rho(r)$ varies with the degree of multiple bonding, but it does have to be calibrated against other systems with the same atom constituents; in other words, it is a relative rather than absolute index. The bond ellipticity ε, which is a measure of the deviation of the electron density distribution from cylindrical symmetry, has also been used[8] in an empirical sense to distinguish between a double bond (for which ε has typical values of 0.4−0.8) and a triple or single bond (where it is close to zero). The Laplacian $\nabla^2\rho(r)$ is a more interesting metric[9] related to the kinetic and potential energy densities at the BCP. Thus, negative values of $\nabla^2\rho(r)$ together with a high value for $\rho(r)$ are normally associated with a lowering of the potential energy and of covalent character in the bonding region. Positive values for $\nabla^2\rho(r)$ are indicative of excess kinetic energy density over potential energy density (i.e., $2G(r) > |V(r)|$, where $G(r)$ is the kinetic energy density and $V(r)$ the potential energy

* Corresponding author e-mail: rzepa@imperial.ac.uk.

10.1021/ct100470g
Published on Web 12/09/2010

Table 1. Calculated Properties for 1, CS, and HCS^+ [a]

system	C−S length (Å), $\nu_{CS}(cm^{-1})$ [b]	AIM: $\rho(r)_{C-S}$; $\nabla^2\rho(r)$, ε [c]	ELF, C−S basin integral (electrons) [d]	NBO E2 (kcal/mol), Wiberg bond order [e]	digital repository [f]
HC≡S$^+$	1.4902, 1403	0.275; +0.723, 0.00	3.53 [g]	-, 2.94	10042/to-3617 10042/to-3661
1, X = OTf	1.4898 [h],1393	0.283; +0.618, 0.022 [h]	2.60	-, -, --, 2.67	10042/to-3628 10042/to-5102
C=S	1.5505, 1269	0.276; +0.226, 0.00	2.73	-, 2.70	10042/to-3616 10042/to-5107
1, X = F	1.5273, 1272	0.278; +0.150, 0.261	2.62	-, 2.44	10042/to-3624 10042/to-3654
1, X = Cl	1.5352,1244	0.272;+0.163, 0.196	2.68	119.3,2.38	10042/to-3622 10042/to-3655
1, X = HO	1.5549, 1205	0.272; −0.114, 0.380	2.62	44.0, 2.27	10042/to-3627 10042/to-3653
1, X = H_2N	1.5889, 1010/1131	0.267; −0.460, 0.459	2.39	24.5, 2.05	10042/to-5199 10042/to-5200
1, X = CN	1.6322, 842/1040	0.250; −0.575, 0.126	1.94	17.5, 1.81	10042/to-3638 10042/to-5106
1, X = H_2B	1.7110, 814	0.221; −0.436, 0.052	1.89	6.1, 1.54	10042/to-3625 10042/to-3662
CH_3SH	1.8255, 719	0.178; −0.278, 0.09	1.60	-, 1.04	10042/to-3615 10042/to-5105

[a] An interactive version of this table is available via the HTML version of this article. Display requires a Java-enabled Web browser, 3D models, and 2D diagrams being invoked by clicking on any of the labeled buttons or pull-down menus in the left-hand navigation window. The resulting Jmol display can also be controlled by a pull down menu produced by a right-mouse click in the right-hand viewing window, from which individual coordinate files can also be acquired. [b] CCSD(T)/cc-pVTZ, calculated using Gaussian 09, Rev A.02. [c] Calculated at the CCSD/cc-pVTZ level using natural orbitals with the programs AIMALL V. 9.10.17 (aim.tkgristmill.com/) and AIM2000 (www.aim2000.de/). BCPs as shown as small purple spheres, and ring critical points as larger yellow spheres. The value of $\rho(r)$ at the critical point is shown as an attached label. [d] ELF function η calculated at the CCSD/cc-pVTZ level using CCSD(T)/cc-pVTZ geometries, with natural orbitals (density = cc keyword) and the program TopMod09 (ref 12). The basin integrations are shown as attached labels, with the basin centroids shown as small magenta spheres. [e] NBO interaction energy (kcal mol^{-1}) between LP(carbon) and BD. * (S-X), calculated using B3LYP/cc-pVTZ wave functions at CCSD(T)/cc-pVTZ geometries for the NBO population analysis and the Wiberg bond index of the C−S bond. [f] OAI-PMH compliant Digital repository identifier, resolved as e.g. http://dx.doi.org/10042/to-2494. [g] Using TopMod09, a single ELF basin for the CS bond is identified, having a centroid located along the bond, with the total basin integration shown. Using DGrid-4.5, the ELF function is identified as a torus, with multiple basin centroids distributed around the center line of the torus but resulting in the same total integration. [h] Geometry optimized at the B3LYP/cc-pVTZ level and the wave function calculated at the CCSD/cc-pVTZ level.

density) and indicate either ionic or charge-shift character.[10] Ionic bonds, which experience closed-shell Pauli (also known as overlap or exchange) repulsions are associated with the contraction of electrons toward an atom and a low value for $\rho(r)$ at the BCP. In contrast, charge-shift bonds retain high values for $\rho(r)$, and bond stabilization for this latter type of bond is thought to originate from resonance terms between charge-shifted or ionic valence-bond forms and the (potentially repulsive) covalent form.[10]

A related approach is adopted for the (closed shell) ELF technique.[3,4,11,12] The wave function is used to compute an electron localization function η, which is normalized between values of 0.0 and 1.0.[3] This empirical function is based on comparing the additional kinetic energy density due to the Pauli principle at any point with that of a homogeneous electron gas (for which $\eta = 0.5$). By contouring the function at different isosurface thresholds, one can systematically locate the domains in η, and these can then be associated with either core electrons (which are referred to as attractors) or the valence electrons. The diatomic valence bonding regions are referred to as disynaptic basins (trisynaptic basins can also exist, and correspond to three-center bonds) and the nonbonding ones as monosynaptic basins. These basins can then be integrated for $\rho(r)$ to give an estimate of the electron population for each bond or lone pair, and from that an estimate of the bond order.[11]

The level of theory adopted here is the CCSD(T)/cc-pVTZ coupled cluster approach used previously,[1] all geometries being fully optimized at this level using Gaussian 09.[13] Full computational details and results are available via the digital repository entries listed in the Table 1. The AIM properties and ELF function were computed at the CCSD level using natural orbitals. The original ELF approach was reformulated for Kohn−Sham wave functions by Savin et al.[14] and more recently Silvi and co-workers have presented an extension to correlated and/or multireference methods.[12] This latter approach, implemented in the TopMod09 program has been used here, employing the CCSD method. The results are displayed in the online interactive Table 1 for a variety of different substituents X for species **1**, and also for three calibrants, CH_3SH, CS, and its protonated form HC≡S$^+$. The reason for including the latter is that in the limiting case where X is highly electron withdrawing (a good nucleofuge), species **1** dissociates to HCS^+ and X^-.

HCS^+ itself, being at one extreme of the series investigated (the other extreme being CH_3SH) in this analysis reveals itself to have something close to a C≡S triple bond. The bond length for this molecule is the shortest by a significant margin, the Wiberg bond order is almost 3, and the C≡S vibration mode at 1403 cm^{-1} is easily the highest (it had been previously demonstrated[1] that the CCSD(T)/cc-pVTZ method matches experiment very well indeed in this regard). Of the AIM indices, $\rho(r)$ has a relatively high value of 0.275 au and ε is zero, as it must be for a linear triple bond. For comparison, $\rho(r)$ for ethyne calculated at the same level is 0.418 au. The triflate **1**, X = OTf, in which the S−O bond

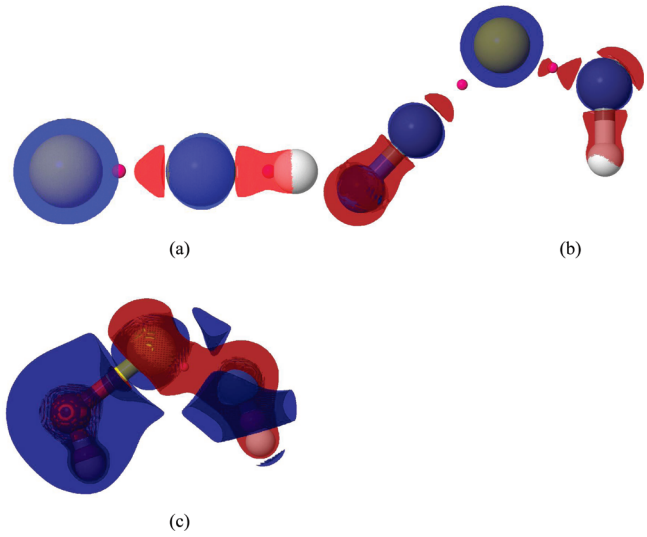

Figure 1. Isosurface computed at CCSD/cc-pVTZ for (a) the computed Laplacian $\nabla^2\rho(r)$ for HCS^+ contoured at +0.723 (blue surface) and −0.723 (red surface). (b) $\nabla^2\rho(r)$ for **1**, X = CN contoured at +0.575 (blue surface) and −0.575 (red surface). (c) $\nabla^2\rho(r)$ for **1**, *X* = OH. Purple spheres are again indicative of the positions of BCPs.

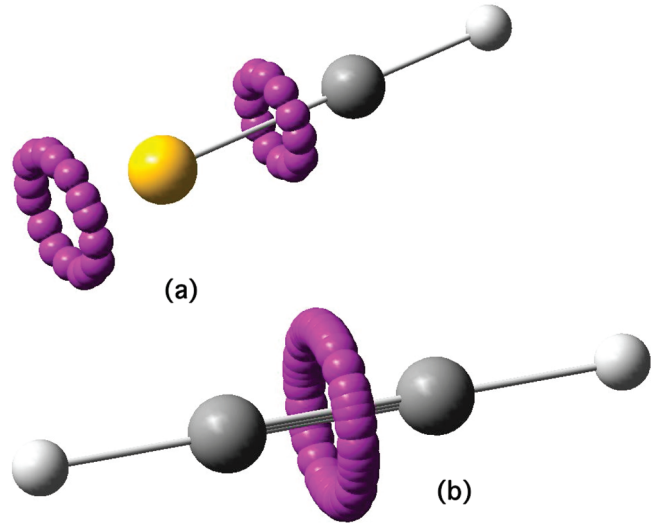

Figure 2. Analysis of the ELF function for (a) HCS^+ and (b) HCCH. The centroids of the ELF localization domains (purple spheres) trace out the center line of torus encircling the CS or CC bond and (for HCS^+) the terminal lone pairs. The finite number of centroids seen in the diagram is purely a function of the resolution chosen for the cube of ELF values.

is largely ionic, resembles HCS^+ fairly closely (Table 1). The substituents **1**, X = F, Cl are however significantly attenuated from the triflate in $\nabla^2\rho(r)$ and **1**, X = OH (the species reported by Schreiner and co-workers[1]) continues this trend. Even more extreme attenuation can be achieved by using, e.g., the electropositive substituent **1**, X = BH_2. Here it is apparent that the C−S bond is only slightly stronger that a pure C−S single bond as exhibited by CH_3SH. The C−S bond ellipticity ε reaches a maximum in the series for **1**, X = H_2N (0.47); X = OH is somewhat reduced (0.38) indicating possibly the incursion of some triple bond character with this substituent (thus the description originally proposed[1] of it having a weak C≡S triple bond seems justified).

A large and positive value for the Laplacian $\nabla^2\rho(r)$ is calculated for HCS^+ (+0.723); this combination of large values for both $\rho(r)$ and $\nabla^2\rho(r)$ has been suggested as a characteristic of the charge-shift bond type recently highlighted by Shaik and Hiberty.[10] The Laplacian $\nabla^2\rho(r)$ across the entire series changes from positive (+0.618 for **1**, *X* = TfO) to negative (−0.575 for **1**, X = CN) implying a dramatic change in character of this bond from charge-shift to covalent induced by a mere neutral substituent X! The value of $\nabla^2\rho(r)$ for **1**, *X* = OH (−0.114) is at the crossover between the C−S bond having charge-shift and having covalent character. However, one must remember that the association between positive values of the Laplacian $\nabla^2\rho(r)$ and the valence-bond-computed bond stabilization deriving from resonance terms between charge-shifted VB structures and (more repulsive) covalent VB forms, as described by Hiberty and Shaik,[10] was largely derived from studies of homonuclear bonds from the first row. Less is known about such associations for second period elements such as sulfur.

To illustrate how care has to be taken in interpreting $\nabla^2\rho(r)$, the calculated isosurface for this property contoured at $\nabla^2\rho(r)$ = 0.723 (the value at the coordinate of the C−S BCP) is shown in Figure 1a for HCS^+ (an interactive version of this and other surfaces and coordinates is available via Table 1 in the HTML version of this article). The blue isosurface in the figure represents the positive Laplacian and is conventionally associated with (electrophilic) regions of charge depletion; the red surface represents the negative Laplacian and is associated with (nucleophilic) regions of charge accumulation. Typically, charge depletion occurs from the valence shells of atoms and the accumulation is found in the bonds. The BCP for the C−S bond of HCS^+ is typically displaced along the C−S axis away from the midpoint and toward the more diffuse distribution of the second period sulfur atom (Figure 1, see centroids of the purple spheres), where it encounters the charge-depleted region of the S valence shell. The C−S bond nonetheless does have a (red) region of charge accumulation, but this resides much closer to the carbon atom and does not envelope the bond-critical point. In contrast, the bond-critical coordinate of the C−H bond is displaced toward the hydrogen (reflecting the much smaller density around H and because as a general rule the BCP tends to be closer to the more electropositive atom of the bond), where it is contained within the region of negative (red) Laplacian.

A wider perspective can be obtained by comparing these results for HCS^+ with other systems. Discussing first **1**, *X* = CN, the calculated Laplacian $\nabla^2\rho(r)$ has a value (−0.575) for the C−S BCP which is at the negative extreme of the systems studied (Figure 1b). The electronic impact of substituent X has been to move the C−S BCP coordinate away from the sulfur, and toward the now more electropositive carbon. At this position, the BCP is now contained within the region of C−S bond charge accumulation, as suggested by the negative sign of the Laplacian at that point. The next system **1**, X = OH shows a value for $\nabla^2\rho(r)$ at the C−S BCP that is numerically small (+0.114, Figure 1c) and which reveals more complex features for the $\nabla^2\rho(r)$ isosur-

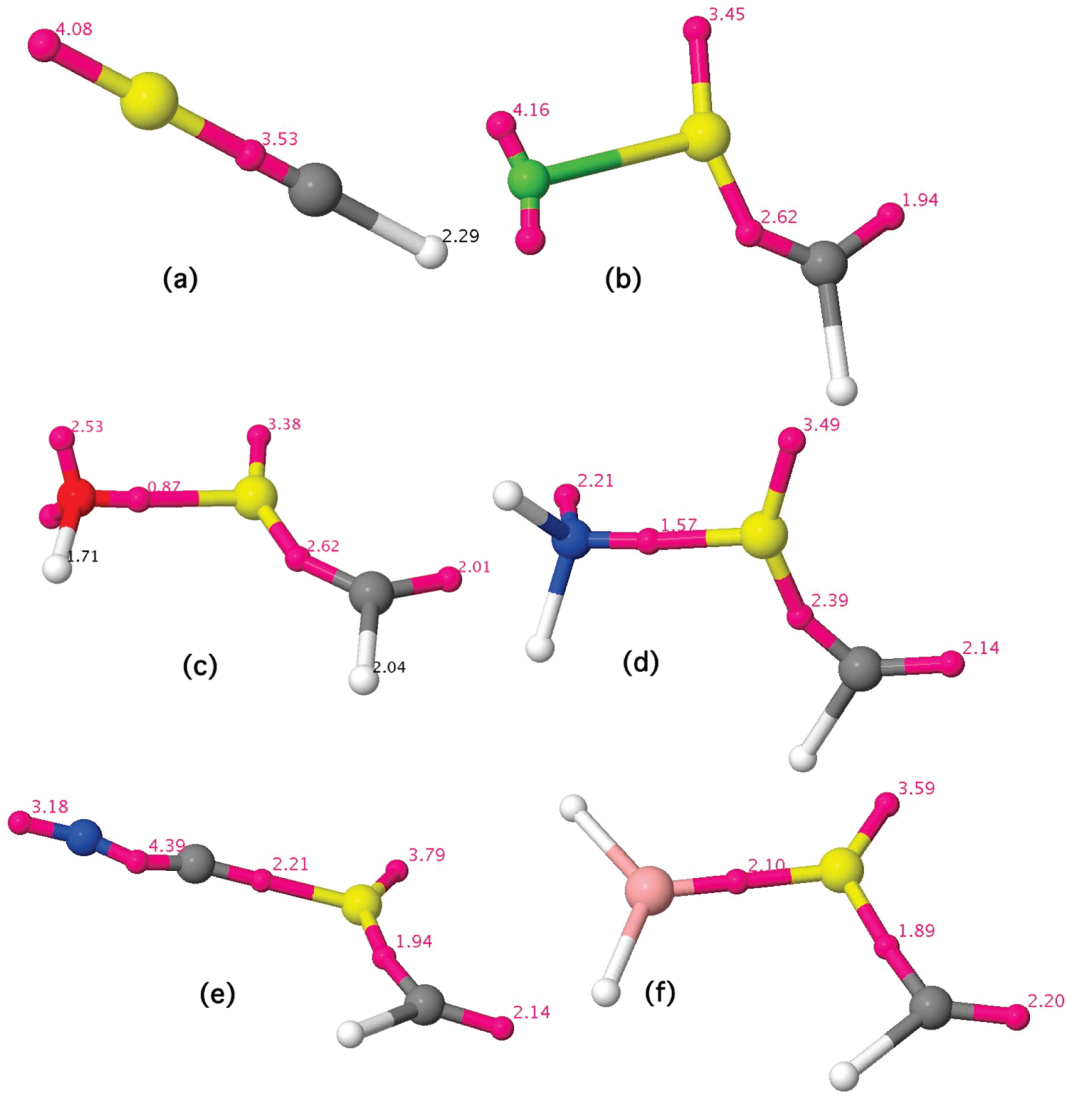

Figure 3. ELF basin centroids (purple spheres) and basin electron populations calculated at the CCSD/cc-pVTZ level for (a) HCS^+, (b) **1**,X = F, (c) **1**,X = OH, (d) **1**,X = NH_2, (e) **1**,X = CN, and (f) **1**,X = BH_2.

face. The BCP is now located in a region where $\nabla^2\rho(r)$ is itself changing sign (in effect $\nabla^3\rho(r)$ is large) but the C−S bond itself is wrapped in a (red) torus of negative charge accumulation that spans both the bond and the adjacent lone pairs on C and S. The final discussion in this perspective relates to the pair **1**, X = NH_2 and X = BH_2, which (at first sight surprisingly) present rather similar $\nabla^2\rho(r)$ values at the C−S BCP (Table 1), despite the very different nature of the two substituents. This is due to a combination of the shape of the $\nabla^2\rho(r)$ isosurface and the actual position of the BCP. For X = BH_2, the BCP is more or less at the midpoint of the C−S bond, displaced very slightly toward the C, whereas with X = NH_2 the BCP is markedly displaced away from the midpoint toward the S. This only serves to indicate that the value of $\nabla^2\rho(r)$ at the BCP itself may not represent the character of the bond as a whole.

One may conclude from these trends that, unlike (homonuclear) bonds between first period elements, the sign of the Laplacian at the BCP for bonds involving a combination of first and second period element may not necessarily represent a simple measure of the degree of covalency or charge-shift character in that bond.

The ELF analysis of these systems adds several further insights to the bonding. The form of the ELF valence localization domains for the C≡S and sulfur lone pair regions of the axially symmetric species HCS^+ take the form of a **torus** encircling the CS bond (Figure 2) with a radius of ∼0.33 Å and second torus of radius 0.45 Å representing the S lone pairs. Ethyne itself[4] gives an ELF torus with radius 0.48 Å (Figure 2b) for the C≡C region which integrates to a population of 5.11 electrons. The total is less than the nominal six electrons for a triple bond because some absorption takes place into the carbon core attractors (∼0.1 each) and the C−H basins (∼0.35 each). Integration of the ELF torus encircling the CS bond in HCS^+ for ρ(r) yields a population of 3.53e, reduced from the nominal triple-bond population of six due to relocation of ∼0.3e into the CH basin, and ∼1.87e into the terminal sulfur lone pair region (Figure 2a). A similar reduction is found for, e.g., N_2, for which the N≡N basin population is reduced to ∼3.57e by transfer occurring from the π region to the terminal lone pairs (3.11e each).

If the axial symmetry is destroyed, then the ELF function avoids the toroidal form of the localization domain, and

instead collapses into two or more[4] conventional disynaptic basins, depending on the symmetry. For the systems **1**, the perturbation by substituent X causes the carbon−sulfur localization domain to bifurcate into two such separate basins, one being disynaptic and localized into the axis of the CS bond (Figure 3). A second (formally disynaptic) basin is more biased toward the carbon and therefore tends to being a monosynaptic carbene "lone pair". Several associated trends are worth highlighting:

1. The population of the X−S basin is the most variable, ranging from zero (a significantly ionic bond, the covalent population being absorbed into lone pairs on X), through 0.87 (semi-ionic, X = OH), to ∼2.1−2.2 (covalent, X = BH_2, CN).

2. The population of the disynaptic C−S basin modestly decreases with decreasing electronegativity of X, from 2.62 (X = F) to 1.89 (X = BH_2).

3. The population of the second "carbene" basin remains relatively constant (1.94−2.20).

4. The sum of the C−S and "carbene" populations (4.63 for X = OH) is rather greater than that of the original unbifurcated triple bond C−S basin in HCS^+ itself (3.53). This is mostly due to scavenging of the sulfur lone pair population (4.08 for HCS^+ is reduced to 3.38 for X = OH).

5. Groups such as X = CN have a more complex interplay between the σ and π frameworks, overall tending to an electropositive manifestation for X.

This bifurcation (Figure 3) also now offers an opportunity to provide some insight into why this CS bond is so tunable across such a wide range (Table 1), from close to a triple bond (X = OTf) to being a single bond with X = BH_2. An NBO analysis[15] (of the DFT density) reveals the carbene basin ("Lp" in NBO terminology) to have a hugely variable interaction energy (Table 1) with the S−X BD* antibonding acceptor. The geometric alignment between the axis connecting the C to the centroid of the carbon basin, and the axis of the S−X bond is almost perfectly antiperiplanar; a classic anomeric effect in fact! One might also note another smaller anomeric alignment between the C−H bond as acceptor and the monosynaptic basin on the sulfur as donor (E2 interaction energy 7.8 kcal mol^{-1}). These interactions were not identified for comment in the original NBO analysis.[1]

For some substituents such as **1**,X = OTf or F, the S−X bond is so ionic that this term is not presented in the NBO analysis[1] (another manifestation of the absorption of the ELF disynaptic basin away from the S−X region for these molecules onto the monosynaptic oxy-anion lone pairs of X, as noted earlier). In the other direction, the disynaptic S−X bond basin integration reaches a maximum of 2.10e for **1**,X = BH_2, with a concomitant reduction to 1.89e for the C−S bond. The actual molecule **1**,X = OH that provoked this entire discussion is intermediate between these extremes; the S−X basin has a small population 0.87e (typical of a partially ionic bond) and the C−S basin integrates to 2.62e (some way off the maximum of 3.53e for the CS toroidal localization domain achieved by the fully ionised HCS^+ itself). The reduction in the CS basin integral is due to the bifurcation of the erstwhile triple bond basin into 2.01e that have split off to form a carbon "lone pair", leaving 2.62e behind in the CS region proper. This former density is perfectly oriented to achieve stabilization by an anomeric-style interaction with the S−X (antiperiplanar) acceptor bond.

This mechanism thus reveals the C−S "bond" in such systems to comprise two separate electronic components as identified by the ELF technique, the partitioning of which enables the high degree of tunability of the bond order. The QTAIM properties, and in particular the Laplacian at the C−S bond critical-point, also show considerable variation with the nature of group X. A full valence-bond analysis of these systems would be needed to establish if the C−S bond exhibits charge-shift character. A search identifying other molecules containing such tunable bonds may be a worthwhile endeavor.

Acknowledgment. The author thanks Philippe Hiberty, Sason Shaik, and Bernard Silvi for many helpful discussions.

References

(1) Schreiner, P. R.; Reisenauer, H. P.; Romanski, J.; Mloston, G. *Angew. Chem.* **2009**, *48*, 8133–8136, DOI: 10.1002/anie.200903969.

(2) (a) Bader, R. F. W. *Atoms in Molecules: A Quantum Theory*; Oxford University Press: Oxford, UK, 1990; (b) Popelier, P. L. A., *Atoms in Molecules: An Introduction*; Prentice-Hall: London (2000); (c) Poater, J.; Duran, M.; Sola, M.; Silvi, B. *Chem. Rev.* **2005**, *105*, 3911–3947. (d) Bader, R. F. W. *J. Phys. Chem.* **2010**, *114*, 7431–7444, DOI: 10.1021/jp102748b.

(3) Becke, A. D.; Edgecombe, K. E. *J. Chem. Phys.* **1990**, *92*, 5397–5403, DOI: 10.1063/1.458517.

(4) (a) For a wide ranging early review of the applications of this technique, see: Savin, A.; Nesper, R.; Wengert, S.; Fassler, T. E. *Angew. Chem., Int. Ed.* **1997**, *36*, 1808–1832, DOI: 10.1002/anie.19971808. For representative recent applications, see: (b) Berski, S.; Latajka, Z.; Gordon, A. J. *J. Chem. Phys.* **2010**, *133*, DOI: 10.1063/1.3460593. (c) Brock, D. S.; de Pury, J. J. C.; Mercier, H. P. A.; Schrobilgen, G. J.; Silvi, B. *J. Am. Chem. Soc.* **2010**, *132*, 3533–3542, DOI: 10.1021/ja9098559. (c) Contreras-Garcia, J.; Pendas, A. M.; Recio, J. M.; Silvi, B. *J. Chem. Theory Comput.* **2009**, *5*, 164–173, DOI: 10.1021/ct800420n. (d) Gotz, K.; Kaupp, M.; Braunschweig, H.; Stalke, D. *Chem.—Eur. J.* **2009**, *15*, 623–632, DOI: 10.1002/chem.200801073. (e) Grabowsky, S.; Hesse, M. F.; Paulmann, C.; Luger, P.; Beckmann, J. *Inorg. Chem.* **2009**, *48*, 4384–4393, DOI: 10.1021/ic900074r. (f) Jubert, A.; Okulik, N.; Michelini, M. D.; Mota, C. J. A. *J. Phys. Chem. A* **2008**, *112*, 11468–11480, DOI: 10.1021/jp805699x. (g) Lein, M. *Coord. Chem. Rev.* **2009**, *253*, 625–634, DOI: 10.1016/j.ccr.2008.07.007. (h) Matito, E.; Sola, M. *Coord. Chem. Rev.* **2009**, *253*, 647–665, DOI: 10.1016/j.ccr.2008.10.003. (i) Trujillo, C.; Mo, O.; Yanez, M.; Silvi, B. *J. Chem. Theory Comput.* **2008**, *4*, 1593–1599, DOI: 10.1021/ct800178x. (j) Vidal, I.; Melchor, S.; Dobado, J. A. *J. Phys. Chem. A* **2008**, *112*, 34143423 DOI: 10.1021/jp075370p. (k) Polo, V.; Andres, J.; Silvi, B. *J. Comput. Chem.* **2007**, *28*, 857–864, DOI: 10.1002/jcc.20615. (l) Mo, O.; Yanez, M.; Pendas, A. M.; Del Bene, J. E.; Alkorta, I.; Elguero, *J. Phys. Chem. Chem. Phys.* **2007**, *9*, 3970–3977, DOI: 10.1039/B702480K.

(5) Rzepa, H. S. *Nat. Chem.* **2009**, *1*, 510–512, DOI: 10.1038/nchem.373.

(6) Bachrach, S. The C-S triple bond. URL:http://comporgchem.com/blog/?p=510. Accessed: 2010−04−20. (Archived by WebCite® at http://www.webcitation.org/5p8JYMMba).

(7) (a) Rzepa. H. S. The nature of the C'S triple bond. URL: http://www.ch.ic.ac.uk/rzepa/blog/?p=1210. Accessed: 2010−04−20. (Archived by WebCite® at http://www.webcitation.org/5p8Jp1zNh); (b) Rzepa, H. S. The nature of the C'S Triple bond: Part 2. URL:http://www.ch.ic.ac.uk/rzepa/blog/?p=1243. Accessed: 2010−04−20. (Archived by WebCite at http://www.webcitation.org/5p8KGaf5n); (c) Rzepa, H. S. The nature of the C'S triple bond: part 3. URL:http://www.ch.ic.ac.uk/rzepa/blog/?p=1278. Accessed: 2010−04−20. (Archived by WebCite at http://www.webcitation.org/5p8KMlrLF).

(8) For a succinct definition and discussion of these properties, see Rode, J. E.; Dobrowolski, *J. Chem. Phys. Lett* **2007**, *449*, 240–245, DOI: 10.1016/j.cplett.2007.10.048.

(9) For a useful definition and discussion of this property, see: Kobayashi, K.; Nagaser, S. *Chem. Phys. Lett.* **1999**, *302*, 312–316, DOI: 10.1016/S0009−2614(99)00135−9.

(10) (a) Shaik, S.; Danovich, D.; Wu, W.; Hiberty, P. C. *Nature Chem.* **2009**, *1*, 443–449, DOI: 10.1038/nchem.327. (b) Shaik, S.; Danovich, D.; Silvi, B.; Lauvergnat, D. L.; Hiberty, P. C. *Chem.—Eur. J.* **2005**, *11*, 6358–6371, DOI: 10.1002/chem.200500265.

(11) (a) Savin, A. *J. Chem. Sci.* **2005**, *117*, 473–475, DOI: 10.1007/BF02708351. (b) Chamorro, E.; Fuentealba, P.; Savin, A. *J. Comput. Chem.* **2003**, *24*, 496–504, DOI: 10.1002/jcc.10242.

(12) Feixas, F.; Matito, E.; Duran, S. M.; Silvi, B. *J. Chem. Theory Comp.* **2010**, *6*, 2736−2742.

(13) *Gaussian 09, Revision A.2*, Frisch, M. J., Trucks, G. W., Schlegel, H. B., Scuseria, G. E., Robb, M. A., Cheeseman, J. R., Scalmani, G., Barone, V., Mennucci, B., Petersson, G. A., Nakatsuji, H., Caricato, M., Li, X., Hratchian, H. P., Izmaylov, A. F., Bloino, J., Zheng, G., Sonnenberg, J. L., Hada, M., Ehara, M., Toyota, K., Fukuda, R., Hasegawa, J., Ishida, M., Nakajima, T., Honda, Y., Kitao, O., Nakai, H., Vreven, T., Montgomery, Jr., J. A., Peralta, J. E., Ogliaro, F., Bearpark, M., Heyd, J. J., Brothers, E., Kudin, K. N., Staroverov, V. N., Kobayashi, R., Normand, J., Raghavachari, K., Rendell, A., Burant, J. C., Iyengar, S. S., Tomasi, J., Cossi, M., Rega, N., Millam, N. J., Klene, M., Knox, J. E., Cross, J. B., Bakken, V., Adamo, C., Jaramillo, J., Gomperts, R., Stratmann, R. E., Yazyev, O., Austin, A. J., Cammi, R., Pomelli, C., Ochterski, J. W., Martin, R. L., Morokuma, K., Zakrzewski, V. G., Voth, G. A., Salvador, P., Dannenberg, J. J., Dapprich, S., Daniels, A. D., Farkas, Ö., Foresman, J. B., Ortiz, J. V., Cioslowski, J., Fox, D. J. Gaussian, Inc.: Wallingford CT, 2009.

(14) (a) Savin, A.; Jepsen, O.; Flad, J.; Andersen, O. K.; Preuss, H.; von Schnering, H. G. *Angew. Chem. Int. Ed.* **1992**, *31*, 187–188, DOI: 10.1002/anie.199201871. (b) Silvi, B.; Savin, A. *Nature* **1994**, *371*, 683–686, DOI: 10.1038/371683a0. (c) Kohout, M.; Savin, A. *J. Comput. Chem.* **1998**, *18*, 1431–1439, DOI: 10.1002/(SICI)1096−987X(199709)18:12 < 1431::AID-JCC1 > 3.0.CO;2-K.

(15) Weinhold, F. Landis, C. R. *Valency and Bonding: A Natural Bond Orbital Donor-Acceptor Perspective*; Cambridge University Press: New York, 2005, pp 760.

CT100470G